Food Chemistry 460 (2024) 140718

Contents lists available at ScienceDirect

Food Chemistry

journal homepage: www.elsevier.com/locate/foodchem

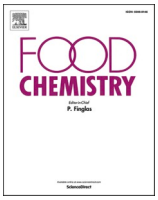

Unrevealing the potentialities in food formulations of a low-branched dextran from *Leuconostoc mesenteroides*

Giulia Bisson [a], Sofia Melchior [a], Clara Comuzzi [a], Francesco Andreatta [b], Alfredo Rondinella [b], Matteo Zanocco [b], Sonia Calligaris [a], Marilena Marino [a,*]

[a] Department of Agricultural Food Environmental and Animal Science, Via Sondrio 2/A, 33100, University of Udine, Udine, Italy
[b] Polytechnic Department of Engineering and Architecture, Via delle Scienze 206, 33100, University of Udine, Udine, Italy

ARTICLE INFO

Keywords:
Dextran
Leuconostoc mesenteroides
Antimicrobial
Antioxidant
Gel-like behavior

ABSTRACT

The search for novel exopolysaccharides (EPS) with targeted functionalities is currently a topic of great interest. This study aimed to investigate the chemical characteristics and technological properties of a novel EPS (named EPS_O) from *Leuconostoc mesenteroides*. EPS_O was a high-molecular-weight dextran (>6.68 × 10^5 g/mol) characterized by high water-holding capacity (785 ± 73%) and high water solubility index (about 99%). EPS_O in water (<30 mg/mL) formed viscous solutions, whereas at concentrations >30 mg/mL, it formed weak gels. Notably, lower concentrations (4–5 mg/mL) exhibited antimicrobial activity against various foodborne pathogens, antibiofilm activity against *Listeria monocytogenes*, and radical-scavenging activity. These properties are significant for maintaining food quality and promoting health. Based on these findings, EPS_O presents itself as a promising food ingredient that could elevate food quality and confer health benefits to consumers.

1. Introduction

The demand for natural polymers for various industrial applications has sparked interest in microbial exopolysaccharides (EPS). EPS are high-molecular-weight (Mw) polymers synthesized during fermentation by various microorganisms (bacteria, fungi, and algae). Among them, several lactic acid bacteria (LAB) genera, mainly *Lactobacillus*, *Lactococcus, Leuconostoc*, *Weissella*, and *Streptococcus* spp., are renowned for their EPS production. In recent years, microbial-derived EPS have increasingly been used to improve the texture and rheological properties of food, due to their solubility, water retention capacity, and ability to act as thickeners. Although these polymers are primarily used in the dairy industry, they can also find applications in other food sectors. For instance, they are applied to improve the creaminess in yogurt-like products, increase the loaf volume in gluten-free bread, and enhance the textural properties of fermented sausages (Wang et al., 2018).

Leuconostoc spp. is reconized for producing homopolysaccharides (HoPS), particularly dextrans (Bisson et al., 2023). Dextran is a chain of glucose units that are linked together by α-(1,6) bonds, with varying degrees of branching at α-(1,2), α-(1,3), and α-(1,4) positions (Maina et al., 2014). Dextrans produced by *Leuconostoc* spp. find several industrial applications as carriers, encapsulants, and thickeners. The technological properties of dextrans depend on their structural characteristics, such as Mw, branching degree, and bond type. Distinctive characteristics are closely linked to the specific strain and fermentation conditions, resulting in unique dextran compositions. Dextrans with branching degrees ranging from 4% to 26%, produced by various strains of *Leuconostoc mesenteroides* displayed diverse gel-forming capabilities. The prevalence of branching showed an inverse correlation with both gel-forming ability and solubility (Diana et al., 2019). The diverse structural composition of polymers provides an advantage across various technological applications as thickener and gelling agents, as well as for moisture retention in semi-fluid (i.e. milk, soups), viscous (i.e. creams, yogurts) and semi-solid (i.e. doughts and breads) products. In addition to altering rheological properties, they can enhance the stability of food products through their antimicrobial, antibiofilm, and antioxidant properties (Yilmaz et al., 2022). It is worth noting that these attributes suggest their potential application as health-enhancing ingredients.

While there is now a considerable body of literature on dextrans due to their significant potential in food formulations - improving rheological properties, food stability, and health benefits – there is an ongoing need for further research in this field. This includes identifying new sources of EPS to further enhance their potential in food applications.

* Corresponding author at: Department of Agricultural Food Environmental and Animal Science, University of Udine, via Sondrio 2/A, 33100 Udine, Italy.
E-mail address: marilena.marino@uniud.it (M. Marino).

https://doi.org/10.1016/j.foodchem.2024.140718
Received 16 January 2024; Received in revised form 17 July 2024; Accepted 29 July 2024
Available online 31 July 2024

Additionally, there is limited information available on studies that simultaneously examine the technological functionalities and bioactivities of a specific dextran for use in foods and within the human body (Xing et al., 2018; Yilmaz et al., 2022). Therefore, the primary aim of this study was to investigate the potential of a novel EPS from *Leuc. mesenteroides*, focusing on both these aspects alongside comprehensive chemical characterization to identify possible correlations.

2. Materials and methods

2.1. Microorganisms and chemicals

Leuc. mesenteroides strain DSA_O was isolated from an Italian raw milk cheese and identified by partial 16S rRNA gene amplification using the primers P1V1 and P4V3 (Klijn et al., 1991). The strain was stored in de Man Rogosa Sharpe (MRS) broth containing 30% glycerol (*v*/v) at −80 °C. Overnight cultures were obtained by inoculating 1 mL of MRS broth with a loop of the cryopreserved stock culture followed by an overnight incubation at 30 °C. *Staphylococcus aureus* DSA 226, *Salmonella enterica* spp. *arizonae* DSMZ 9386, *Escherichia coli* DSA 8048, *Listeria monocytogenes* Scott A, *Enterococcus faecium* DMSZ 2146 and L. *monocytogenes* DSA 248 were stored at −80 °C in Brain Heart Infusion (BHI) containing 30% (*v*/v) glycerol. The overnight culture was prepared for each pathogen by inoculating 1 mL of BHI with a loop of the cryopreserved stock culture followed by incubation at 37 °C overnight.

MRS broth, Maximum Recovery Diluent (MRD), Bacteriological peptone, Lab-Lemco powder, BHI broth, and yeast extract were purchased from Oxoid, Ltd. (Milan, Italy). Mayeux Sandine Elliker agar (MSE) was acquired from Biolife Italiana s.r.l. (Milan, Italy). Acetonitrile (≥ 99.9%), ascorbic acid (≥ 98%), Crystal violet and Phosphate Buffered Saline (PBS), 2,2-azino-bis-(3-ethylbenzo-thiazoline-6-sulfonic acid) diammonium salt (ABTS; purity ≥98%), 2,2-diphenyl-1-picrylhydrazyl (DPPH), potassium persulfate (ACS reagent ≥99%), ammonium citrate tribasic (≥ 97%), D-(−)-fructose (≥ 99%), D-(+)-glucose (≥ 99.5%), D-(+)-sucrose (≥ 99.5%), deuterium oxide (D_2O; 99.9%), dextran analytical standards (nominal Mw 1.16×10^3; 4.86×10^4; 8.09×10^4; 1.48×10^5; 4.10×10^5; 6.68×10^5 g/mol), glycerol (for molecular biology ≥99.0%), magnesium sulfate heptahydrate (ACS reagent ≥98%), manganese sulfate tetrahydrate (≥ 99.5%), 96% sulfuric acid, trichloroacetic acid (TCA; ACS reagent ≥99%), 3-(Trimethylsilyl)-1-propanesulfonic acid sodium salt (DSS; 97%), sodium acetate trihydrate (ACS reagent ≥99%), and sodium hydroxide (ACS reagent ≥97%) where purchased from Sigma-Aldrich Chemical Co., Ltd. (St. Louis, MO, USA).

Absolute ethanol, potassium dihydrogen phosphate (ACS reagent ≥99%), and dipotassium hydrogen phosphate (ACS reagent ≥99%) were obtained from Carlo Erba Reagents s.r.l. (Milan, Italy). Tween 80 was purchased from Liofilchem s.r.l. (Teramo, Italy).

Pierce™ Bradford Protein Assay Kit was purchased from Thermo Fisher Scientific (Waltham, MA, USA).

2.2. EPS production, purification, and quantification

To obtain EPS_O, 1 L of MRS-S broth (Bacteriological peptone 10 g/L, Lab-Lemco powder 8 g/L, yeast extract 4 g/L, D-(+)-sucrose 20 g/L, dipotassium hydrogen phosphate 2 g/L, sodium acetate trihydrate 5 g/L, ammonium citrate tribasic 2 g/L, magnesium sulfate heptahydrate 0.2 g/L, manganese sulfate tetrahydrate 0.05 g/L, Tween 80 1 mL/L, pH adjusted to 6.2 ± 0.2 before sterilization at 121 °C for 15 min) was inoculated at 1% (*v*/v) with the overnight culture of *Leuc. mesenteroides* (prepared as described in section 2.1) and then incubated at 25 °C for 48 h in aerobic conditions. EPS_O was recovered and purified following the method of Dilna et al. (2015) with slight modifications. TCA 4% (*w*/*v*) was added to the broth and left for 30 min at 4 °C under stirring. Then the culture broth was centrifuged at 13,000 x*g* for 10 min at 4 °C in an Avanti Centrifuge™ J-25 (Beckman Coulter, Indianapolis, Indiana, USA). The supernatant was added with three volumes of cold (4 °C) absolute ethanol and kept at 4 °C overnight. The pellet was recovered and washed three times with cold (4 °C) absolute ethanol by centrifugation at 13,000 x*g* for 10 min at 4 °C, resuspended in 50 mL of Milli-Q water, and dialyzed in a Slide-A-Lyzer Dialysis Casette with Mw cut-off 10,000 g/mol (Thermo Fisher Scientific). 1.5 L of Milli-Q water was used as dialysis buffer. The sample was dialyzed for 3 h at 4 °C, then the Milli-Q water was replaced and the sample was dialyzed for another 3 h at 4 °C. The dialysis buffer was then replaced and the sample was dialyzed overnight. EPS_O was freeze-dried (Epsilon 2–4 LSCplus, Martin Christ Gefriertrocknungsanlagen GmbH, Osterode am Harz, Germany) setting the vacuum pressure at 0.8 mBar and the condenser temperature at −45 °C. The freeze-dried sample was stored under vacuum at room temperature until analysis. EPS_O extraction rate was determined by gravimetry.

2.3. Chemical characterization

The UV–Vis spectrum of EPS_O was acquired by a Varian Cary 50 spectrophotometer (Agilent Technologies, Santa Clara, CA, USA). EPS_O solution (2.5 mg/mL) was prepared by dissolving EPS_O in water and shaking with Vortex 1 (Ika, Milan, Italy) for 2 min, until complete solubilization.

EPS_O functional groups were analyzed using an Alpha-P(ATR)-Fourier transform infrared (FTIR) spectroscope (Bruker Optics, Milan, Italy). The instrument was equipped with an attenuated total reflectance (ATR) device and a Zn—Se crystal, allowing the collection of FT-IR spectra without any sample preparation. 2 mg of freeze-dried EPS_O were placed on the Zn—Se crystal of the ATR device and pressed by a pointed tip to ensure uniformity in the surface area of contact between the crystal and the sample. FT-IR spectra were acquired in the range from 4000 to 400 cm^{-1}, at a spectra resolution of 4 cm^{-1}, and with 32 coadded scans.

The protein content of EPS_O solution (2 mg/mL) was determined using the Pierce™ Bradford protein assay kit (Thermo Fisher Scientific) according to the manufacturer's instructions, and the protein content was expressed as a percentage.

Monosaccharide composition was analyzed as described by Dilna et al. (2015) with slight modifications. In a 10-mL Pyrex® tube, 20 mg of EPS_O were added with 2 mL of sulfuric acid 1 M, incubated at 100 °C for 2 h in a Jouan EU145 oven (Jouan-SA, Saint-Herblain, France), and then neutralized by adding sodium hydroxide 2 M. The hydrolyzed sample was analyzed by high-performance liquid chromatography (HPLC) using a 1260 Infinity HPLC system (Agilent Technologies) equipped with auto-injector (1260 ALS), a quaternary pump autosampler (1260 Quat Pump), a refractive index detector, a temperature control system (1260 TCC) and a chromatographic column (Ultra Amino 100 A; 250 mm, 4.6 mm internal diameter, 5 μm) (Restek s.r.l., Cernusco sul Naviglio, Italy) set at 25 °C. The mobile phase was an acetonitrile/Milli-Q water mixture (70:30, *v*/v), the flow rate was 1.0 mL/min and the injection volume was 20 μL. A solution containing D-(−)-fructose (0.05 g/mL), D-(+)-glucose (0.05 g/mL) and D-(+)-sucrose (0.05 g/mL) was used as standard.

The Mw of EPS_O was determined by size-exclusion high-performance liquid chromatography (HPLC-SEC) as described by Zhou et al. (2018) with slight modifications. As previously reported (Bisson et al., 2023) the following setup was used: the instrument was composed by a LC250 binary pump (Perkin Elmer, Waltham, MA, USA) a Rheodyne injector (Rohnert Park, CA, USA) and a RID-10 A refractive index detector (Shimadzu, Milan, Italy). Separation columns were Ultrahydrogel 250 (6 μm, 300 × 7.8 mm) (Waters Corporation, Milford, MA, USA) and a PL-aquagel-OH MIXED-H (300 × 7.5 mm, 8.0 μm) (Agilent Technologies) connected in series and working at room temperature. EPS_O solution (2.5 mg/mL) was prepared by dissolving EPS_O in Milli-Q water and letting it solubilize for 1 h at room temperature under stirring. Then the solution was filtered using a 0.45 μm mixed cellulose esters (MCE) syringe filter (Artiglass s.r.l., Padua, Italy). The injection volume was 20 μL. The elution buffer was Milli-Q water, and the flow rate was 0.6 mL/

min. The approximate Mw was estimated using a calibration curve built with Polyethylene oxide/glycol Easy Vials Mw standards (6.1×10^2, 1.5×10^4, 1.3×10^5, and 1.5×10^6 g/mol; Agilent Technologies). The chromatograms were acquired and analyzed using the software GC Solution MFC Application version 2.4.0.0 (Shimadzu).

The chemical structure of EPS_O was analyzed on a Bruker Avance III 400 MHz digital Nuclear Magnetic Resonance (NMR) spectrometer (Bruker, Karlsruhe, Germany). 5 mg of EPS_O were dissolved in 0.6 mL of D_2O, and ^1H and ^{13}C Distorsionless Enhancement by Polarization Transfer Including the Detection of Quaternary Nuclei (DEPTQ), homonuclear Correlated Spectroscopy (COSY), and Heteronuclear Single Quantum Coherence (HSQC) NMR experiments were performed at 25 °C. DSS was used as an external standard. Chemical shifts were expressed as part per million (ppm).

NMR Diffusion Ordered Spectroscopy (DOSY) experiments were used to estimate the Mw of the polysaccharide (Maina et al., 2014). A calibration curve was made dissolving 2 mg of each dextran analytical standard in 0.6 mL of D_2O. The DOSY experiments were conducted by adjusting, in each sample, the pulse sequence parameters (δ, Δ). The molecular diffusion coefficient (D) was calculated using the Stejskal-Tanner Eq. (1):

$$I = I_0 exp\left[(\gamma \times g \times \delta)^2 \times \left(\Delta - \frac{\delta}{3}\right) \times D\right] \quad (1)$$

where g is the gradient strength (g/cm), Δ is the diffusion delay (s), D is the diffusion coefficient (cm^2/s), δ is the gradient length (s), I is the observed spin-echo intensity, I_0 is the intensity of the analog experiment performed without gradients and γ the magnetogyric constant (rad/Gs) of the nucleus whose phase is encoded/decoded by the gradients. The dextran standards' D values (m^2/s) were correlated to Mw according to the following Eq. (2):

$$D = KMw^{\alpha} \quad (2)$$

The exponential equation was $D = 7.283 \times 10^{-9}$ $Mw^{-0.496}$ in agreement with a previous report (Viel et al., 2003). Applying the same protocol, the diffusion coefficient was estimated, and the Mw was calculated using the exponential equation from the calibration curve.

2.4. Scanning electron microscopy (SEM)

The morphology of EPS_O was examined using an EVO 40 scanning electron microscope (Carl Zeiss, Milan, Italy) equipped with energy-dispersive X-ray spectroscopy (EDXS). To prevent the formation of artifacts, samples were stored in a desiccator with silica beads and taken immediately before analyses to avoid hydration.

The samples were mounted on an electrically conductive, non-porous carbon tape, which served as support for the SEM-EDXS characterization. A thin Au layer was sputter coated on the EPS_O on the supporting C tape to minimize sample electric charging and improve secondary electron emission during the analysis. Secondary-electron images were captured at various magnifications (up to 5000×). EDXS spectra were collected at different locations of the sample surface to qualitatively evaluate the chemical composition. SEM images and EDXS spectra were acquired with an acceleration voltage of 20 kV and a working distance of 12 mm. To ensure the images were representative, at least three different areas of each sample were analyzed.

2.5. Antioxidant activity

The 2,2-diphenyl-1-picrylhydrazyl (DPPH) free radical scavenging activity was determined using the method described by Blois (1958). Briefly, 1 mL of EPS_O or ascorbic acid solution at different concentrations (0.5–1–2-4 mg/mL) was mixed with 1 mL of DPPH 0.2 mM ethanolic solution and let in the dark for 30 min. Then the mixture was centrifuged at 7000 xg for 10 min using a D3024 centrifuge (DLAB Scientific Europe S.A.S, Schiltigheim, France). 150 μL of the supernatant were placed in triplicate wells of a U-bottomed 96-well polystyrene microtiter plate (Corning Life Sciences) and the absorbance was read at 517 nm using a Sunrise microplate reader (Tecan s.r.l., Cernusco s. N, Milan, Italy). The DPPH radical inhibition (%) was calculated using the following Eq. (3):

$$\%DPPH\ radical\ inhibition = (A_0 - A_t/A_0) \times 100 \quad (3)$$

where A_0 is the absorbance of the DPPH solution and A_t is the absorbance of the sample.

The [2,2′-azinobis-(3-ethylbenzothiazoline-6-sulfonate)] (ABTS) radical scavenging activity was measured using the method of Re et al. (1999). A stock solution of ABTS 7.4 mM and 2.3 mM potassium persulfate was prepared and kept in the dark for 12 h. The solution was then diluted with Milli-Q water to reach an absorbance of 0.70 ± 0.02 at 734 nm which was read using an EnSight microplate reader (Perkin Elmer, Milan, Italy). In each well of a U-bottomed 96-well polystyrene microtiter plate (Corning Life Sciences), 30 μL of the ABTS solution were added with 170 μL of EPS_O or ascorbic acid solution at different concentrations (0.5–1–2-4 mg/mL). After 10 min the absorbance (734 nm) was read using an EnSight microplate reader and the % of ABTS radical inhibition was measured using the following Eq. (4):

$$\%ABTS\ radical\ inhibition = (A_0 - A_t/A_0) \times 100 \quad (4)$$

where A_0 is the absorbance of the control and A_t is the absorbance of the sample.

2.6. Antimicrobial activity

The antimicrobial activity of EPS_O was tested against *S. aureus* DSA 226, *Salm. enterica* spp. *arizonae* DSMZ 9386, *E. coli* DSA 8048, *L. monocytogenes* Scott A, and *Ent. faecium* DMSZ 2146 using a turbidimetric approach. Before the analysis, for each pathogen, an overnight culture was prepared by inoculating 1 mL of BHI broth with a loop of the cryopreserved stock culture and incubated at 37 °C. After centrifugation at 13,000 xg for 5 min (Mikro 20 centrifuge; Hettich Italia s.r.l., Milan, Italy), the supernatant was discarded and cells were washed twice with 1 mL of MRD and diluted (1:100) with MRD to reach a cell concentration of about 10^6 CFU/mL. Duplicate wells of a U-bottomed 96-well polystyrene microplate (Corning Life Sciences) were filled with 190 μL of BHI broth containing EPS_O (1.25, 2.5, and 5 mg/mL). BHI containing EPS_O was prepared by adding the EPS to BHI broth and shaking it on a Vortex 1 for 2 min. Each well was inoculated with 10 μL of each microbial culture and the microplate was incubated at 37 °C for 48 h. Wells containing inoculated BHI broth were used as control (CTRL) and wells containing non-inoculated BHI as blank. Optical Density (OD) measurements were recorded every 30 min using a Sunrise microplate reader. The growth kinetics were modeled using the Growth Curve Analysis Tool (GCAT) according to the Gompertz equation (Bukhman et al., 2015) Eq. (5):

$$y = Aexp\{-exp[\mu_{max} \times e/A(\lambda - t) + 1]\} \quad (5)$$

where t is time (h), y is the log-transformed OD value, A is the upper asymptote (amplitude), μ_{max} is the maximum specific growth rate (Log OD/h), and λ is the lag phase (h).

2.7. Inhibition of biofilm formation by L. monocytogenes

The inhibition of biofilm formation by *L. monocytogenes* DSA 248 was tested using the method described by Stepanović et al. (2000). Overnight culture of L. *monocytogenes* DSA 248 was prepared by inoculating 1 mL of BHI broth with a loop of the cryopreserved stock culture and incubating it at 37 °C. Then, cells were recovered from 1 mL overnight culture by centrifugation at 13,000 xg for 5 min (Mikro 20 centrifuge).

The resulting pellet was washed three times with 1 mL of MRD and then diluted with MRD to reach a cell concentration of about 10^6 CFU/mL. Duplicate wells of a polystyrene flat-bottomed 96-well microtiter plate (Corning Life Sciences) were filled with 10 µL of the cell culture and 190 µL of BHI broth containing 2.5 and 5 mg/mL of EPS_O. To ensure that EPS_O was completely solubilized, the BHI containing the EPS was shaken on a Vortex 1 for 2 min until complete solubilization of the EPS. Wells containing inoculated BHI broth were used as control (CTRL), and non-inoculated wells as blank. Microplates were incubated for 24 h at 37 °C to allow biofilm formation on the bottom of the flat well. After incubation, wells were emptied by carefully inverting the microplate. The biofilm was washed twice with 300 µL of PBS, then wells were emptied and the microplate was dried at 60 °C for 30 min (Maifreni et al., 2023). The biofilm was then stained with 150 µL of 2% (*v*/v) crystal violet for 30 min at 25 °C, then crystal violet was removed and the biofilm was fixed with 150 µL of cold (4 °C) absolute ethanol. After 30 min the absorbance at 570 nm was read using a Sunrise microplate reader.

2.8. Water solubility index (WSI)

The WSI of EPS_O was determined as described by Wang et al. (2010). 50 mg of EPS_O was added with 1 mL of distilled water and kept under stirring for 2 h at room temperature to form a uniform suspension. After centrifugation at 13,000 x*g* for 30 min in a D3024 centrifuge the supernatant was collected and dried at 100 °C for 4 h using a Memmert UF55 plus oven (Memmert, Schwabach, Germany). The Water Solubility Index (WSI) was then calculated according to Eq. (6):

$$WSI(\%) = (m_0 - m_1/m) \times 100 \quad (6)$$

where m_0 is the weight of the dry supernatant and m_1 is the weight of EPS_O.

2.9. Water holding capacity (WHC)

WHC was assessed following the method of Wang and Kinsella (1976). Freeze-dried EPS_O (50 mg) was suspended in 1 mL of Milli-Q water, shaked on a Vortex 1 and centrifuged at 13,000 x*g* for 30 min at 20 °C. The supernatant was discarded, and the pellet was weighed on an analytical balance. The WHC was calculated through the following Eq. (7):

$$WHC\ (\%) = \frac{H - FDS}{FDS} * 100 \quad (7)$$

where FDS is the weight (g on dry basis) of freeze-dried EPS_O and H is the weight of pellet obtained after centrifugation and supernatant removal (g).

2.10. Rheological properties

EPS_O was solubilized in Milli-Q water at concentrations from 10 to 70 mg/mL. Resulting systems were characterized using a controlled Haake RheoStress 6000 stress rheometer (Thermo Scientific, Karlsruhe, Germany) equipped with a Peltier system and parallel plate geometry (35 mm diameter, 1 mm gap). The flow behavior was measured by recording shear stress values when shearing the samples at an increasing shear rate from 0.01 to 200 s^{-1}. Data were fitted using the Power Law model reported in Eq. (8):

$$Power\ Law\ \sigma = K\gamma^n \quad (8)$$

where σ (Pa) is the shear stress, γ (s^{-1}) is the shear rate, K (Pas^n) is the consistency coefficient; n is the flow behavior index. The linear viscoelastic region was detected by the stress sweep test at increasing stress from 0.1 to 100 Pa at 1 Hz frequency. Frequency sweep tests were performed at 20 °C by increasing the frequency from 0.1 to 10 Hz using a fixed stress value included in the linear viscoelastic region.

2.11. Statistical analysis

All trials were carried out at least in duplicate and values expressed as the means ± SD. One-way Analysis of Variance (ANOVA) and Tukey's-HSD *post-hoc* test were performed to evaluate the significance of differences among means ($p < 0.05$) using R v.4.1.2 for Windows (The R foundation for statistical computing).

3. Results and discussion

3.1. EPS_O production, purity, and chemical characterization

Leuc. mesenteroides strain DSA_O was able to form mucous and slimy colonies on MSE agar plates (Fig. S1). After extraction and purification from liquid media, the extraction rate of EPS_O was 3.84 g/L, consistent with previous findings for this microbial species (Li et al., 2020). The chemical, technological, and biological features of EPS can be affected by the presence of contaminants (e.g., proteins, nucleic acids), so the purity of EPS_O was the initial focus of the assessment. The separation of EPS from culture broths can yield an impure product, especially in terms of protein content, as EPS may create a network in which proteins remain embedded, preventing their precipitation after treatment with TCA. In this study, the UV–Vis spectrum (Fig. 1a) did not display any peaks at 260 nm, indicating the absence of proteins (Yang et al., 2018). To further explore potential protein contamination, EPS_O underwent a Bradford assay, which revealed a protein content <0.05%. Similarly, no DNA contamination was detected as evidenced by the absence of peaks at 260 nm (Fig. 1a).

The FT-IR spectrum showed different peaks in the region between

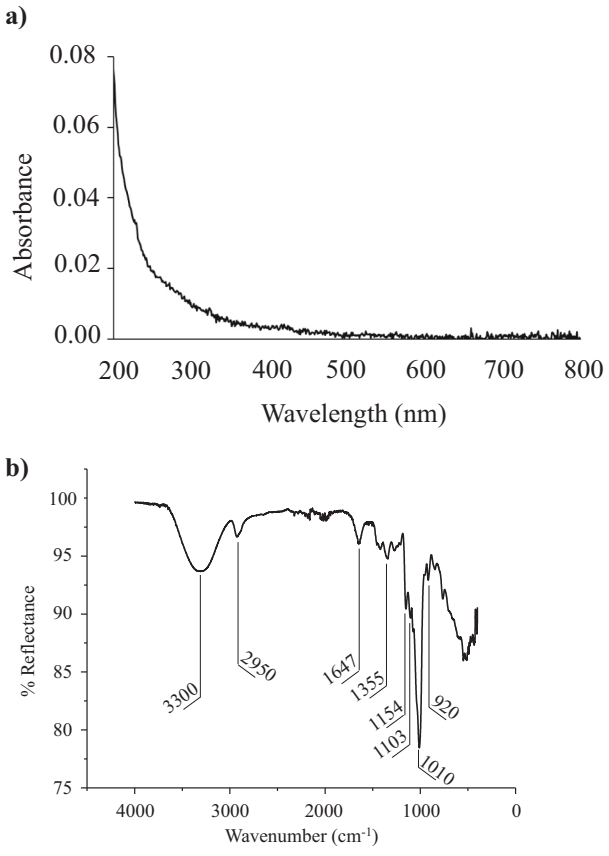

Fig. 1. UV–Vis spectrum profile (a) and FT-IR spectrum detected in the range of 400–4000 cm^{-1} (b) of EPS_O.

3400 and 500 cm^{-1} (Fig. 1b).

The wide absorption peak at 3300 cm^{-1} corresponded to the stretching vibrations of the hydroxyl group (O—H), whereas the peak at 2950 cm^{-1} could be attributed to C—H stretching vibration (Yang et al., 2018). A narrow peak at 1647 cm^{-1} was associated with the presence of water. The band at 1154 cm^{-1} corresponded to the vibrations of the C-O-C bond and the glycosidic bridge, while the one at 1355 cm^{-1} was related to C-OH bond vibrations. The peak at 1103 cm^{-1} corresponded to the vibration of the C—O bond at the C-4 position of glucose residue while the peak at 1010 cm^{-1} was due to the chain flexibility around α (1 → 6) bond. The presence of α-glycosidic bond was indicated by a peak at 920 cm^{-1} (Purama et al., 2009). No peaks referring to proteins, such as amide I and amide II bands, were detected, confirming the absence of protein contamination.

Monosaccharide composition analysis was carried out by HPLC. A comparison of data from EPS_O hydrolysis and different standards indicated that the purified EPS_O was composed solely of glucose units (Fig. S2), suggesting that EPS_O could be a dextran. It was previously reported that *Leuc. mesenteroides* can produce dextran type EPS (Purama et al., 2009).

The ^{1}H NMR and ^{13}C-DEPTQ NMR spectroscopy of EPS_O are depicted in Fig. 2. The ^{1}H NMR spectra revealed the presence of two signals in the anomeric region. The peak at 4.9 ppm was attributed to the presence of α-(1 → 6) linked glucose units while a low-intensity anomeric signal at 5.3 ppm was assigned to the α-(1 → 3) linkages, consistent with those found in other dextrans produced by *Lactobacillus mali* CUPV271 and *Leuconostoc carnosum* CUPV411 (Llamas-Arriba et al., 2019).

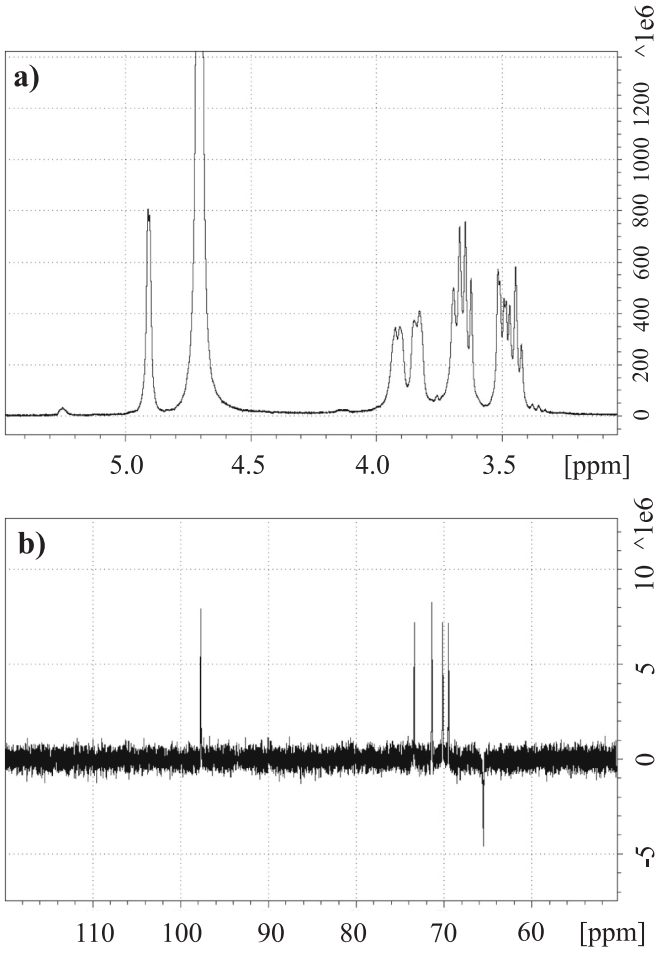

Fig. 2. a) ^{1}H and b) ^{13}C-DEPTQ NMR spectra of EPS_O produced by *Leuc. mesenteroides* DSA_O.

The heteronuclear HSQC spectra evidenced the α anomeric nature of the signals of EPS_O since a cross peak at δH-1/δC-1 = 4.9/97.7 ppm was detected (Fig. S3). Moreover, the ^{13}C–DEPTQ and HSQC evidenced the main resonance at 65.5 ppm as the C-6 carbon, which was involved in the glycosidic linkage as highlighted by the ^{13}C chemical shift. The signals in the range of 69.5–73.4 were assigned to the bulk signals through homonuclear COSY (Fig. S4) as previously reported (Llamas-Arriba et al., 2019). The integration of the ^{1}H signals of the anomeric region indicated that EPS_O had a low degree of α-(1 → 3) branching (<5%), and no signals of the branching linkage to the backbone were detectable in ^{13}C HSQC spectra. The molecular weight (Mw) of EPS_O was determined using HPLC-SEC and NMR-DOSY, which was previously successfully applied to evaluate the Mw of dextrans (Maina et al., 2014). Regarding the HPLC SEC analysis, the Mw range of the columns used was rather wide (10^{3}- 6 × 10^{6} g/mol), since the Mw of EPS and in particular dextrans can vary based on the microbial species and producing strain (Du et al., 2018). The DOSY experiments revealed that the Mw of EPS_O exceeded 6.68 × 10^{5} g/mol, which was the highest Mw of the dextran standard used for the calibration curve. Furthermore, the estimated diffusion coefficient (D value) suggested a Mw significantly higher than 10^{6} g/mol, approaching the technique's limit. This finding was corroborated by HPLC-SEC analysis (Fig. S5), which revealed that EPS_O had an Mw exceeding the scale of the standards used and higher than the upper Mw limit of the column (6 × 10^{6} g/mol). This result is in line with previous reports. Indeed, the production of high Mw dextran by *Leuconostoc* spp. has already been reported (Bisson et al., 2023; Yilmaz et al., 2022; Zhou et al., 2018). The synthesis of high Mw EPS is considered of interest since high-Mw EPS plays a crucial role in enhancing the formation of the EPS-protein network structure and improving the texture of the fermented products (Wang et al., 2018). It should be noted that analyzing the structural and macromolecular properties of high molecular weight dextrans can be challenging due to their complex architecture (Maina et al., 2014). However, further analysis should be carried out to determine the exact Mw of EPS_O.

3.2. Scanning electron microscopy

SEM is a powerful technique for elucidating the surface morphology of EPS upon freeze-drying. The microstructure and surface morphology of EPS_O at different magnifications are illustrated in Fig. 3. The images revealed that EPS_O was characterized by irregular flakes with a smooth surface and a web-like structure (Fig. 3a and b). The presence of small pores (Fig. 3c and d) on the surface was likely associated to water removal during freeze-drying.

The structure of EPS_O close resembled the dextran synthesized from *Leuconostoc pseudomesenteroides*, and an EPS produced by *Leuconostoc citreum* NM105. In contrast, a distinctly different appearance was observed in a dextran produced by *Leuc. mesenteroides* NRRL B-640 which had a more compact and regular structure. This suggests that each microbial strain produces a unique EPS with distinct physicochemical and morphological properties (Purama et al., 2009; Yang et al., 2015). The morphological appearance of EPS_O could provide indications about its structure (e.g., compact, linear, branched, …) that can be correlated to technological properties (e.g., solubility, WHC, OHC, …) (Purama et al., 2009). A web-like structure as observed in this study was related to the ability to retain water and the stability of the gel structure when subjected to external forces (Yang et al., 2015).

3.3. Antioxidant activity

Oxidation can significantly compromise the quality, safety, and nutritional value of food products. This is due to adverse chemical reactions affecting not only fats but also proteins, sugars, and pigments, leading to undesirable changes in flavor, aroma, and appearance. Furthermore, oxidation can diminish the nutritional value of food by altering essential vitamins and fatty acids, and it can also pose safety

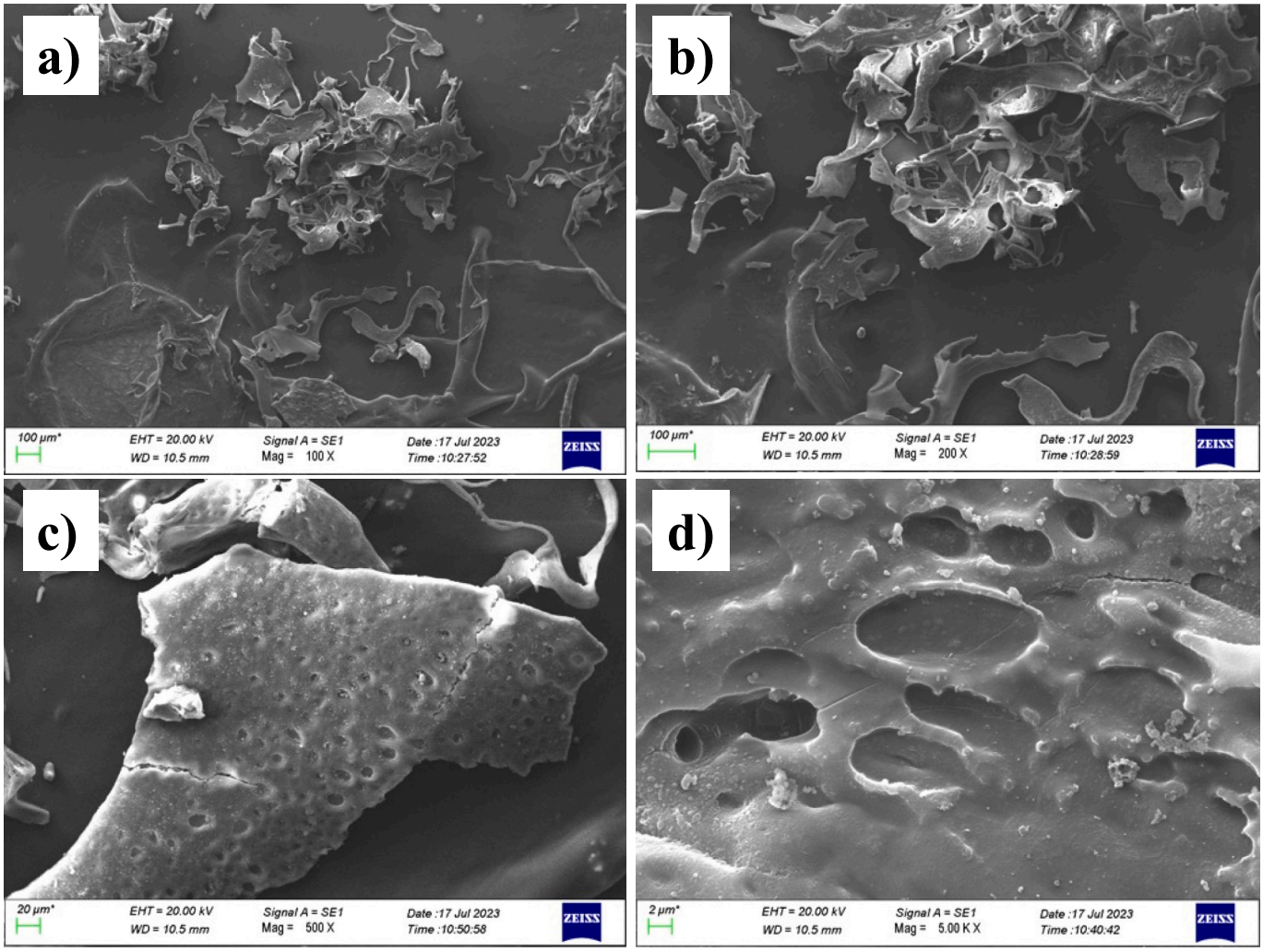

Fig. 3. SEM images of EPS_O at different magnifications; a) 100×, b) 200×, c) 500×, d) 5000 × .

risks through the formation of potentially toxic or carcinogenic compounds. Various antioxidants are commonly used in food products to prevent these reactions. However, some synthetic antioxidants have sparked controversy due to their potential health risks, prompting the search for alternative compounds. It is worth noting that these compounds may also offer physiological benefits, as uncontrolled oxidation can lead to oxidative stress, resulting in significant cellular and molecular damage. This is a key factor in the development and progression of numerous chronic diseases, aging, and overall decline in bodily functions (Shields et al., 2021).

In this study, the antioxidant potential of EPS_O was assessed using DPPH and ABTS assays (Table 1). Both methods involve an electron transfer and the reduction of a colored oxidant. However, it has been reported that the antioxidant ability determined through these *in vitro* methods could differ (Floegel et al., 2011). In both tests, ascorbic acid used as a positive control, exhibited high radical scavenging activity (over 90% and over 80% for DPPH and ABTS, respectively), which remained consistent regardless of the concentration. EPS_O exhibited DPPH scavenging activity, which significantly increased with concentration ($p < 0.05$). At 4 mg/mL, EPS_O had a maximum scavenging rate of 71.33 ± 3.73%, higher than that of other dextran-type polysaccharides produced by *Leuc. pseudomesenteroides* DRP-5 and *Leuc. mesenteroides* BD1710 (about 20% and 40%, respectively) (Du et al., 2018; Xing et al., 2018). The EPS_O exhibited a lower ABTS radical scavenging potential compared to ascorbic acid, with maximum inhibition at 2 mg/mL (24.52 ± 0.34%). However, there was no significant difference in the ABTS radical scavenging potential of different EPS_O concentrations ($p > 0.05$). Similar results were reported for an EPS produced by *Leuc. mesenteroides* SN-8 at the same concentration (Li et al., 2020), whereas a highly branched dextran produced by *Leuc. mesenteroides* BI-20 showed a higher inhibition rate (36.1%) (Yilmaz et al., 2022). Stable radicals such as DPPH and ABTS are reduced by receiving electrons or hydrogen from an antioxidant compound. The type of glycosidic linkages, the presence of glucose units, and the availability of the hydroxyl groups were suggested to affect the

Table 1
The DPPH and ABTS radical scavenging activity (%) of EPS_O and ascorbic acid. For each test, different uppercase letters in the same row indicate different means ($p < 0.05$); different lowercase letters in the same column indicate different means ($p < 0.05$).

	DPPH		ABTS	
Concentration (mg/mL)	Ascorbic acid	EPS_O	Ascorbic acid	EPS_O
0.5	$93.06 \pm 0.34^{a,A}$	$56.37 \pm 1.39^{a,B}$	$83.32 \pm 0.19^{a,A}$	$19.85 \pm 0.93^{a,B}$
1.0	$92.39 \pm 0.19^{a,A}$	$58.73 \pm 1.44^{a,B}$	$83.28 \pm 0.15^{a,A}$	$19.68 \pm 0.77^{a,B}$
2.0	$92.85 \pm 0.44^{a,A}$	$64.78 \pm 3.23^{ab,B}$	$83.53 \pm 0.71^{a,A}$	$24.52 \pm 0.81^{a,B}$
4.0	$92.81 \pm 1.29^{a,A}$	$71.33 \pm 3.73^{b,B}$	$83.55 \pm 0.59^{a,A}$	$21.85 \pm 0.15^{a,B}$

antioxidant properties of polysaccharides (Andrew & Jayaraman, 2020). The antioxidant potential observed in this study for EPS_O could be due to the exposition of the free hydroxyl group. These groups could have donated hydrogen to DDPH and ABTS radicals leading to the formation of their reduced form. Indeed, the radical-scavenging ability of chitosan and dextran was attributed to the presence of hydroxyl groups (Andrew & Jayaraman, 2020). Anyway, the antioxidant potential of EPS_O can be relevant and suggests its possible exploitation in the food field, although the maintenance of the antioxidant effect within foods remains to be further investigated. Other authors have pointed out a possible link between molecular weight and antioxidant activity by highlighting that lower molecular weight EPSs exhibit higher antioxidant activity than higher molecular weight EPS. In addition, the degree of branching also seems to play a key role in determining the antioxidant power of EPS, as it was observed that a dextran with a branching degree of 20% possessed strong antioxidant capabilities (Andrew & Jayaraman, 2020; Yilmaz et al., 2022). In contrast, in this work we found some antioxidant activity in an EPS with a high molecular weight and low degree of branching, which suggests that the structural characteristics of polysaccharides play a combined role in determining antioxidant activity. Further investigation is needed to definitively clarify these relationships.

3.4. Antimicrobial activity of EPS_O

The antimicrobial activity of EPS_O was tested through the turbidimetric growth curves and kinetic parameters were compared to control ones. This technique proved effective when combined with growth curve modeling to gather information on the antimicrobial activity of specific substances and the impact of environmental factors on microbial growth (Bisson et al., 2021). Five food-related pathogens were selected as targets (*E. coli*, *Ent. faecium*, *Salm. enterica* subsp. *arizonae*, *S. aureus*, and L. *monocytogenes*), given their relevance as foodborne microbial threats worldwide. EPS_O affected the growth kinetics of almost all strains tested by lengthening the lag phase, reducing the maximum growth rate, and lowering amplitude (i.e., the difference between initial and final OD). As an example, Fig. 4 reports the growth curve of L. *monocytogenes* Scott A in the presence (2.5 and 5 mg/mL) or not (CTRL) of EPS_O. The effect of EPS_O on growth parameters was species-dependent (Table 2). At both concentrations (2.5 and 5 mg/mL) it affected the growth of *E. coli*, significantly increasing the lag phase and decreasing the maximum growth rate ($p < 0.05$), indicating a possible bacteriostatic effect. In the case of the other Gram-negative strain (*Salm. enterica* subsp. *arizonae*), EPS_O appeared to be more effective in inhibiting growth. At 5 mg/mL, the maximum growth rate and amplitude significantly decreased ($p < 0.05$) passing from 0.25 ± 0.01 log OD/h and 1.32 ± 0.01 OD to 0.19 ± 0.03 log OD/h and 0.76 ± 0.01 OD, respectively. Additionally, the lag phase was significantly longer than in the control sample ($p < 0.05$).

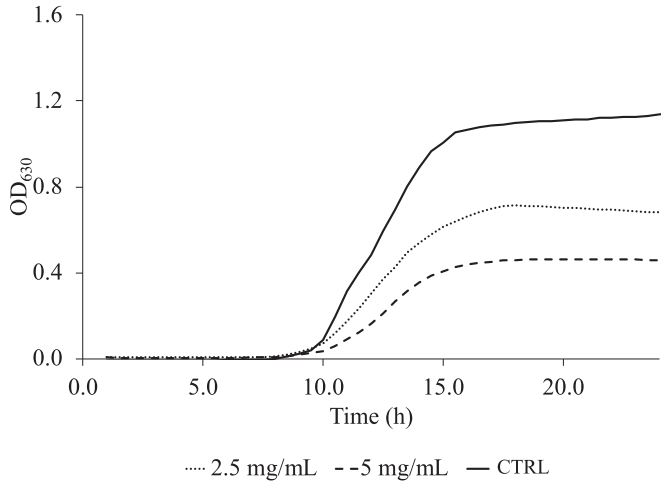

Fig. 4. Turbidimetric growth curves of L. *monocytogenes* Scott A in BHI broth (CTRL) eventually added with 2.5 mg/mL and 5 mg/mL of EPS_O.

Table 2
Growth parameters of foodborne pathogens in the presence of EPS_O; for the same parameter, asterisks indicate a significant difference ($p < 0.05$) with respect to the control (CTRL).

Strain	mg/mL	lag (h)	μ_{max} (log OD/h)	amplitude (OD)
E. coli 8048	CTRL	5.65 ± 0.04	0.41 ± 0.02	1.33 ± 0.04
	2.5	6.55 ± 0.06*	0.23 ± 0.01*	1.18 ± 0.02
	5	7.02 ± 0.15*	0.30 ± 0.02*	1.24 ± 0.02
Salm. enterica 9386	CTRL	5.26 ± 0.08	0.25 ± 0.01	1.32 ± 0.01
	2.5	5.21 ± 0.12	0.16 ± 0.08*	0.93 ± 0.01*
	5	5.83 ± 0.01*	0.19 ± 0.03*	0.76 ± 0.01*
L. monocytogenes Scott A	CTRL	9.67 ± 0.05	0.21 ± 0.05	1.09 ± 0.02
	2.5	9.49 ± 0.23	0.12 ± 0.06*	0.75 ± 0.07*
	5	10.25 ± 0.13	0.10 ± 0.05*	0.48 ± 0.03*
Ent. faecium DSM_20477	CTRL	6.20 ± 0.02	0.50 ± 0.07	1.33 ± 0.02
	2.5	6.49 ± 0.70	0.45 ± 0.03	1.15 ± 0.10*
	5	7.10 ± 0.80	0.30 ± 0.02*	1.00 ± 0.06*
S. aureus DSA 226	CTRL	5.90 ± 0.18	0.29 ± 0.01	1.02 ± 0.03
	2.5	7.12 ± 0.50	0.24 ± 0.03	1.12 ± 0.09
	5	7.26 ± 0.16	0.27 ± 0.01	1.09 ± 0.05

L. monocytogenes was the most affected among Gram-positives. The presence of EPS_O significantly reduced its maximum growth rate, and a notable decrease in the amplitude was observed ($p < 0.05$). *L. monocytogenes* is known to cause listeriosis, a foodborne illness with high mortality and hospitalization rates (Gandhi & Chikindas, 2007). Furthermore, its ubiquity allows it to thrive in challenging environments. Therefore, finding new strategies to control it in the food sector could be crucial, and our results support the potential future applications of EPS from LAB as antimicrobials in food production. The amplitude of *Ent. faecium* decreased at both the concentrations tested, whereas the maximum growth rate decreased significantly at 5 mg/mL ($p < 0.05$). Instead, the growth of *S. aureus* was unaffected by the presence of EPS_O. Based on the literature, the antimicrobial activity of EPS from LAB has already been reported, highlighting that each EPS possesses a unique activity. Indeed, an EPS produced by *Lactobacillus reuteri* SHA101 and *Lactobacillus vaginalis* SHA110 exhibited strong antibacterial activity against *E. coli* and *Salmonella Typhimurium* (Rajoka et al., 2019). Moreover, an EPS synthesized by *Lactobacillus kefirofaciens* DN1 showed to be bactericidal against L. *monocytogenes* and *Salm. enteritidis* (Jeong et al., 2017). These results suggest the potential use of EPS_O ensuring food safety and as an alternative treatment for foodborne illnesses. The mechanisms underlying the antimicrobial activity of EPS, particularly HoPS, are not fully understood. It has been hypothesized that they could form a shield around the microbial cells, limiting

the secretion of cell metabolites and increasing the osmolarity inside the cell. Moreover, it was postulated that high Mw EPS could act as antimicrobial agents due to their capacity to enhance the viscosity of the media (Abdalla et al., 2021). The web-like structure observed in the SEM could support this hypothesis, as web-like structures are related to the ability of EPS to form gels. These structures could retain a lot of water and form a shield around the cells.

Viscosity-related bioactivities such as antimicrobial activity, could be promoted as the increasing of chain length can lead to stronger intramolecular properties. Indeed, EPS_O can form weak gels at a concentration > 30 mg/mL (*w/v*) (*vide infra*, section 3.6). However, further studies are required to elucidate the mechanism of the antimicrobial activity of EPS_O on pathogens, focusing on the possible changes in gene expression or investigating the possible structural changes of the bacterial cell wall using microscopy techniques (Jeong et al., 2017).

3.5. Antibiofilm activity of EPS_O

The ability of EPS_O to inhibit biofilm formation was tested against L. *monocytogenes* DSA 284, an already described biofilm-former (Marino et al., 2018). The biofilm formation by L. *monocytogenes* represents a serious issue in the food industry as this pathogen can adhere to food contact surfaces and form biofilms, leading to cross-contamination of food and, consequently, possible foodborne infections in the consumer. As reported in Fig. 5, EPS_O was able to significantly inhibit ($p < 0.05$) biofilm formation by *L. monocytogenes* even at the lowest concentration of EPS_O (2.5 mg/mL). The mechanisms responsible for the antibiofilm activity are still unclear. It has been suggested that EPS may disrupt the surface of bacteria by impeding cell adhesion to surfaces. Another hypothesis is that these molecules could interfere with *quorum sensing* mechanisms (Abdalla et al., 2021). In our study we theorized that the high Mw and viscosity of EPS_O may have prevented the physical adhesion of cells to the surface, or created a physical barrier around the cells, inhibiting the release of signal molecules that are essential for the *quorum sensing* mechanism. In addition, it is known that the ability of microorganisms to adhere to surfaces and form biofilms is related to the interaction between the external structures of the cell (e.g., pili and flagella) and the surface itself. The shielding of the cell surface by EPS_O may have prevented the interaction of the microorganism with the surface and consequently reduced the formation of biofilms. To the best of our knowledge, this study presents some of the earliest data in the literature on the antibiofilm activity of dextrans produced by *Leuc. mesenteroides*. Traditional approaches of biofilm control imply the use of thermal or chemical strategies. However, these methods could have some drawbacks related to the possible adverse impact on food quality, equipment, and human health (Marino et al., 2018). In this context, the continuous research of new antibiofilm strategies is of interest, and these preliminary results on EPS_O could open new perspectives for an in-depth investigation of the possible application of EPS as antibiofilm agents in the food industry.

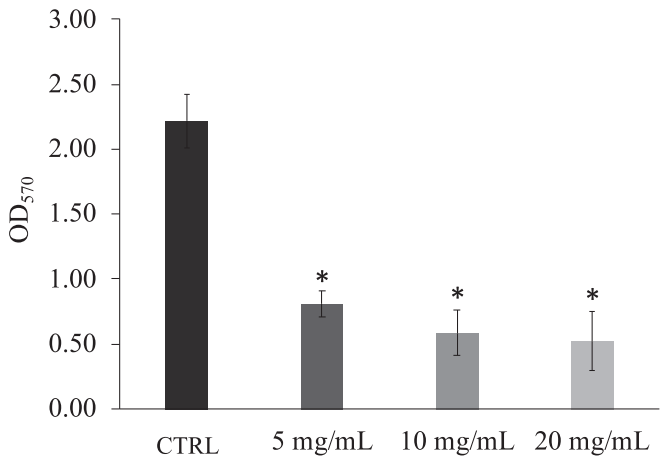

Fig. 5. Antibiofilm activity of different EPS_O concentrations (5, 10 and 20 mg/mL) against L. *monocytogenes* DSA 284.

3.6. Technological properties

The WSI of EPS_O was 99.93% ± 0.02, which could be attributed to the dextran structure. The predominant linear structure of EPS_O, characterized by α-(1 → 6) glycosidic bonds in the main chain, favoured the interaction with water due to the higher exposure of hydroxyl groups (-OH) (Suner et al., 2018). The impact of the structure was reported by other authors for EPS produced by the same microbial species used in this study. For instance, a dextran obtained by *Leuc. mesenteroides* NRRL-B1149 with 52% of α-(1 → 6) and 40% of α-(1 → 3) displayed a low water solubility, which was associated with the presence of a high percentage of α-(1 → 3) linkages while Du et al. (2017) reported high solubility of linear dextran from *Leuc. mesenteroides* TDS2–19. The theory that a linear structure has a positive impact on solubility was corroborated by considering EPS produced by other microorganisms. In this regard, it has been observed that a mainly linear dextran by *Leuc. pseudomesenteroides* XG5 was highly soluble in water (Zhou et al., 2018).

WHC of EPS_O was 785 ± 73%, probably due to the prevalent linear structure of the polymer and to the branched and web-like microstructure as observed by SEM (Fig. 3) which could favor the entrapment of huge water amount through hydrogen bonds (Zhou et al., 2018). EPS_O exhibited a higher WHC compared to other dextrans synthesized by strains belonging to the *Leuconostoc* genus. The dextran produced by *Leuc. mesenteroides* NRRL B-1426 had a WHC of 290%, which was 2.70-fold lower than that of EPS_O (Kothari et al., 2015) while a dextran synthesized by *Leuc. pseudomesenteroides* XG5 exhibited a WHC of 412% (Zhou et al., 2018).

Although some authors reported that the presence of branches favours both solubility and WHC of dextrans due to the better water adsorption and retention of the amorphous areas, our results corroborate the hypotesis that, independently of the Mw, linear molecules are totally soluble (Guo et al., 2017).

In order to througly explore the potential application of EPS_O, we assessed the flow curves of solutions at varying concentrations (Fig. S6). The apparent viscosity of samples decreased by increasing the shear rate due to the breakdown of the structural units of the polysaccharide by hydrodynamic forces, suggesting a shear thinning behavior (pseudoplastic). The latter was also confirmed by the flow index (n) below 1 obtained by fitting the curves with the Power Low model (Table 3). The n values decreased moving from 10 to 20 mg/mL while no differences were detected by further increasing the EPS_O concentration. The increase in EPS_O concentration to 50 mg/mL led to a progressive rise in the consistency index (K) signifying a corresponding elevation in fluid viscosity. This increase potentially exerts a positive influence on

Table 3
Flow behavior (K: consistency coefficient; n: flow behavior), and viscoelastic properties at 1 Hz (storage modulus, G'; loss modulus G") of EPS_O solutions at different concentrations. In the same row, means indicated by different letters are significantly different ($p < 0.05$). nd: not detectable.

EPS mg/mL	K (Pa s^n)	n	R	G' (Pa)	G"(Pa)
10	0.07 ± 0.00^d	0.67 ± 0.02^a	0.995	nd	nd
20	2.14 ± 0.03^c	0.52 ± 0.01^b	0.998	nd	nd
30	3.80 ± 0.49^b	0.46 ± 0.02^b	0.999	23.59 ± 0.13^b	9.72 ± 0.27^c
50	16.84 ± 1.92^a	0.44 ± 0.05^b	0.999	44.26 ± 3.71^a	13.13 ± 0.37^b
70	12.83 ± 2.47^a	0.48 ± 0.02^b	0.999	42.95 ± 3.43^a	19.72 ± 0.38^a

antimicrobial activity (Diana et al., 2019). Pseudoplasticity can be ascribed to both the high Mw and the polymeric structure of EPS_O (Abid et al., 2021; Wang et al., 2019). In this context, it has been demonstrated that high Mw polymers exhibit pseudoplastic behavior compared with low Mw ones (Mw $< 10^5$ g/mol) which show Newtonian behavior with low viscosity (Han et al., 2014). Similar results were observed for other high-Mw ($>10^5$) dextrans produced by *Leuc. mesenteroides* strains (Diana et al., 2019).

The apparent viscosity exhibited a progressive increase with the rise in EPS_O concentration up to 50 mg/mL, with no further alterations noted at 70 mg/mL. These findings may be attributed to the heightened hydrogen bonding with hydroxyl groups. Furthermore, the elevation in concentration led to a reduction in the free movement among molecules, thereby facilitating the formation of intermolecular junctions through crosslinking (Abid et al., 2021). These results were corroborated by dynamic frequency sweep. Samples at 10 and 20 mg/mL exhibited typical viscous fluid properties with the loss modulus (G") higher than the storage modulus (G') in the entire frequency range (data not shown). These results are in accordance with Diana et al. (2019) that observed the same behavior in the case of dextran produced by *Leuc. mesenteroides* at a concentration below 30 mg/mL. On the other hand, at higher concentrations (≥30 mg/mL), the EPS_O systems displayed G' values higher than G" with both moduli frequency-dependent indicating a weak gel behavior. Both G' and G" increased by increasing EPS_O concentration up to 50 mg/mL revealing a higher number of interactions (such as hydrogen bonds and electrostatic interactions) between the closed-pack molecules in highly concentrated solutions, strengthening and stabilizing the gel network (Miao et al., 2015). The correlation between EPS concentration and rheological moduli was documented not only in dextran from *Leuc. mesenteroides* (Abid et al., 2021) but also in other LAB strains, including *Leuc. citreum* BMS (Diana et al., 2019). This behavior was attributed to the heightened number and strength of molecular interactions, which contribute to the formation of additional junction zones. No differences were detected in the 50 and 70 mg/mL solutions probably because the critical concentration was reached. In this condition, it could be supposed that the excess of EPS_O remains in solution without contributing to the network formation.

Overall, rheological properties of EPS_O could be attributed to the Mw as well as the linear structure, thanks to the presence of -OH groups that promote the formation of hydrogen bonds with other molecules.

4. Conclusions

The discovery of new microbial strains that produce unique EPS capable of providing both distinctive technological and health-related benefits to foods is an emerging area of interest today. In this study, EPS_O produced by *Leuc. mesenteroides* DSA_O was identified as a dextran with a Mw $>10^5$ g/mol and a low degree of α-(1 → 3) branching.

EPS_O has shown to possess various versatile features in terms of technological and bioactivity-related functionalities. At high concentrations and depending on the intended application, EPS_O could be used as a thickening agent (<30 mg/mL) or as a gelling agent (>30 mg/mL). Instead, at low concentrations (5 mg/mL) it exhibited radical-scavenging and antimicrobial activity. Moreover, EPS_O effectively inhibited biofilm formation by L. *monocytogenes*, a well-known food-borne pathogen responsible for surface-mediated cross-contamination.

It is possible that the observed antimicrobial and antibiofilm activity against various food-related microbes is linked to the high molecular weight of EPS_O. This high molecular weight allows EPS_O to retain water, leading to the formation of a protective layer around the cells. This layer may result in the excessive accumulation of toxic metabolites near the cell and could also hide adhesion sites on the cell surface. Further investigation will be needed to clarify the mechanisms of these bioactivities, as a comprehensive understanding of the potential of these microbial macromolecules is essential for their targeted application to enhance food quality while providing health benefits to consumers.

Fundings

This research did not receive any specific grant from funding agencies in the public, commercial, or non-profit sectors.

CRediT authorship contribution statement

Giulia Bisson: Writing – original draft, Investigation, Formal analysis. **Sofia Melchior:** Writing – review & editing, Investigation, Formal analysis. **Clara Comuzzi:** Writing – review & editing, Investigation, Formal analysis. **Francesco Andreatta:** Writing – review & editing, Resources, Formal analysis. **Alfredo Rondinella:** Writing – review & editing, Investigation, Formal analysis. **Matteo Zanocco:** Writing – review & editing, Investigation, Formal analysis. **Sonia Calligaris:** Writing – review & editing, Supervision, Resources. **Marilena Marino:** Writing – review & editing, Supervision, Resources, Conceptualization.

Declaration of competing interest

The authors declare that they have no known competing financial interests or personal relationships that could have appeared to influence the work reported in this paper.

Data availability

Data will be made available on request.

Appendix A. Supplementary data

Supplementary data to this article can be found online at https://doi.org/10.1016/j.foodchem.2024.140718.

References

Abdalla, A. K., Ayyash, M. M., Olaimat, A. N., Osaili, T. M., Al-Nabulsi, A. A., Shah, N. P., & Holley, R. (2021). Exopolysaccharides as antimicrobial agents: Mechanism and spectrum of activity. *Frontiers in Microbiology, 12*, Article 664395. https://doi.org/10.3389/fmicb.2021.664395

Abid, Y., Azabou, S., Blecker, C., Gharsallaoui, A., Corsaro, M. M., Besbes, S., & Attia, H. (2021). Rheological and emulsifying properties of an exopolysaccharide produced by potential probiotic *Leuconostoc citreum*-BMS strain. *Carbohydrate Polymers, 256*, Article 117523. https://doi.org/10.1016/j.carbpol.2020.117523

Andrew, M., & Jayaraman, G. (2020). Structural features of microbial exopolysaccharides in relation to their antioxidant activity. *Carbohydrate Research, 487*, Article 107881. https://doi.org/10.1016/j.carres.2019.107881

Bisson, G., Comuzzi, C., Giordani, E., Poletti, D., Boaro, M., & Marino, M. (2023). An exopolysaccharide from *Leuconostoc mesenteroides* showing interesting bioactivities versus foodborne microbial targets. *Carbohydrate Polymers, 301*, Article 120363. https://doi.org/10.1016/j.carbpol.2022.120363

Bisson, G., Marino, M., Poletti, D., Innocente, N., & Maifreni, M. (2021). Turbidimetric definition of growth limits in probiotic *Lactobacillus* strains from the perspective of an adaptation strategy. *Journal of Dairy Science, 104*, 12236–12248. https://doi.org/10.3168/jds.2021-20888

Blois, M. S. (1958). Antioxidant determinations by the use of a stable free radical. *Nature, 181*, 1199–1200. https://doi.org/10.1038/1811199a0

Bukhman, Y. V., di Piazza, N. W., Piotrowski, J., Shao, J., Halstead, A. G. W., Bui, M. D., … Sato, T. K. (2015). Modeling microbial growth curves with GCAT. *Bioenergy Research, 8*, 1022–1030. https://doi.org/10.1007/s12155-015-9584-3

Diana, C.-R., Humberto, H.-S., & Jorge, Y.-F. (2019). Structural characterization and rheological properties of dextran produced by native strains isolated of *Agave salmiana*. *Food Hydrocolloids, 90*, 1–8. https://doi.org/10.1016/j.foodhyd.2018.11.052

Dilna, S. V., Surya, H., Aswathy, R. G., Varsha, K. K., Sakthikumar, D. N., Pandey, A., & Nampoothiri, K. M. (2015). Characterization of an exopolysaccharide with potential health-benefit properties from a probiotic *Lactobacillus plantarum* RJF4. *LWT - Food Science and Technology, 64*, 1179–1186. https://doi.org/10.1016/j.lwt.2015.07.040

Du, R., Qiao, X., Zhao, F., Song, Q., Zhou, Q., Wang, Y., Pan, L., Han, Y., & Zhou, Z. (2018). Purification, characterization and antioxidant activity of dextran produced by *Leuconostoc pseudomesenteroides* from homemade wine. *Carbohydrate Polymers, 198*, 529–536. https://doi.org/10.1016/j.carbpol.2018.06.116

Du, R., Xing, H., Yang, Y., Jiang, H., Zhou, Z., & Han, Y. (2017). Optimization, purification and structural characterization of a dextran produced by *L. mesenteroides* isolated from Chinese sauerkraut. *Carbohydrate Polymers, 174*, 409–416. https://doi.org/10.1016/j.carbpol.2017.06.084

Floegel, A., Kim, D.-O., Chung, S.-J., Koo, S. I., & Chun, O. K. (2011). Comparison of ABTS/DPPH assays to measure antioxidant capacity in popular antioxidant-rich US

foods. *Journal of Food Composition and Analysis, 24*, 1043–1048. https://doi.org/10.1016/j.jfca.2011.01.008
Gandhi, M., & Chikindas, M. L. (2007). *Listeria*: A foodborne pathogen that knows how to survive. *International Journal of Food Microbiology, 113*, 1–15. https://doi.org/10.1016/j.ijfoodmicro.2006.07.008
Guo, M. Q., Hu, X., Wang, C., & Ai, L. (2017). Polysaccharides: Structure and solubility. In Z. Xu (Ed.), *Solubility of polysaccharides* (pp. 7–21). Intech Open Ltd.
Han, J., Hang, F., Guo, B., Liu, Z., You, C., & Wu, Z. (2014). Dextran synthesized by *Leuconostoc mesenteroides* BD1710 in tomato juice supplemented with sucrose. *Carbohydrate Polymers, 112*, 556–562. https://doi.org/10.1016/j.carbpol.2014.06.035
Jeong, D., Kim, D. H., Kang, I. B., Kim, H., Song, K. Y., Kim, H. S., & Seo, K. H. (2017). Characterization and antibacterial activity of a novel exopolysaccharide produced by *Lactobacillus kefiranofaciens* DN1 isolated from kefir. *Food Control, 78*, 436–442. https://doi.org/10.1016/j.foodcont.2017.02.033
Klijn, N., Weerkamp, A. H., & de Vos, W. M. (1991). Identification of mesophilic lactic acid bacteria by using polymerase chain reaction-amplified variable regions of 16S rRNA and specific DNA probes. *Applied and Environmental Microbiology, 57*, 3390–3393. https://doi.org/10.1128/aem.57.11.3390-3393.1991
Kothari, D., Tingirikari, J. M. R., & Goyal, A. (2015). *In vitro* analysis of dextran from *Leuconostoc mesenteroides* NRRL B-1426 for functional food application. *Bioactive Carbohydrates and Dietary Fibre, 6*, 55–61. https://doi.org/10.1016/j.bcdf.2015.08.001
Li, Y., Liu, Y., Cao, C., Zhu, X. Y., Wang, C., Wu, R., & Wu, J. (2020). Extraction and biological activity of exopolysaccharide produced by *Leuconostoc mesenteroides* SN-8. *International Journal of Biological Macromolecules, 157*, 36–44. https://doi.org/10.1016/j.ijbiomac.2020.04.150
Llamas-Arriba, M. G., Puertas, A. I., Prieto, A., López, P., Cobos, M., Miranda, J. I., … Dueñas, M. T. (2019). Characterization of dextrans produced by *Lactobacillus Mali* CUPV271 and *Leuconostoc carnosum* CUPV411. *Food Hydrocolloids, 89*, 613–622. https://doi.org/10.1016/j.foodhyd.2018.10.053
Maifreni, M., di Bonaventura, G., Marino, M., Guarnieri, S., Frigo, F., & Pompilio, A. (2023). Biofilm formation under food-relevant conditions and sanitizers' tolerance of a *Pseudomonas fluorescens* group strain. *Journal of Applied Microbiology, 134*, Article lxad117. https://doi.org/10.1093/jambio/lxad117
Maina, N. H., Pitkänen, L., Heikkinen, S., Tuomainen, P., Virkki, L., & Tenkanen, M. (2014). Challenges in analysis of high-molar mass dextrans: Comparison of HPSEC, AsFlFFF and DOSY NMR spectroscopy. *Carbohydrate Polymers, 99*, 199–207. https://doi.org/10.1016/j.carbpol.2013.08.021
Marino, M., Maifreni, M., Baggio, A., & Innocente, N. (2018). Inactivation of foodborne bacteria biofilms by aqueous and gaseous ozone. *Frontiers in Microbiology, 9*, 2024. https://doi.org/10.3389/fmicb.2018.02024
Miao, M., Huang, C., Jia, X., Cui, S. W., Jiang, B., & Zhang, T. (2015). Physicochemical characteristics of a high molecular weight bioengineered α-D-glucan from *Leuconostoc citreum* SK24.002. *Food Hydrocolloids, 50*, 37–43. https://doi.org/10.1016/j.foodhyd.2015.04.009
Purama, R. K., Goswami, P., Khan, A. T., & Goyal, A. (2009). Structural analysis and properties of dextran produced by *Leuconostoc mesenteroides* NRRL B-640. *Carbohydrate Polymers, 76*, 30–35. https://doi.org/10.1016/j.carbpol.2008.09.018
Rajoka, M. S. R., Mehwish, H. M., Hayat, H. F., Hussain, N., Sarwar, S., Aslam, H., … Shi, J. (2019). Characterization, the antioxidant and antimicrobial activity of exopolysaccharide isolated from poultry origin lactobacilli. *Probiotics and Antimicrobial Proteins, 11*, 1132–1142. https://doi.org/10.1007/s12602-018-9494-8
Re, R., Pellegrini, N., Proteggente, A., Pannala, A., Yang, M., & Rice-Evans, C. (1999). Antioxidant activity applying an improved ABTS radical cation decolorization assay. *Free Radical Biology & Medicine, 26*, 1231–1237. https://doi.org/10.1016/S0891-5849(98)00315-3
Shields, H. J., Traa, A., & van Raamsdonk, J. M. (2021). Beneficial and detrimental effects of reactive oxygen species on lifespan: A comprehensive review of comparative and experimental studies. *Frontiers in Cell and Developmental Biology, 9*, Article 628157. https://doi.org/10.3389/fcell.2021.628157
Stepanović, S., Vuković, D., Dakić, I., Savić, B., & Švabić-Vlahović, M. (2000). A modified microtiter-plate test for quantification of staphylococcal biofilm formation. *Journal of Microbiological Methods, 40*, 175–179. https://doi.org/10.1016/s0167-7012(00)00122-6
Suner, S. S., Sahiner, M., Sengel, S. B., Rees, D. J., Reed, W. F., & Sahiner, N. (2018). Responsive biopolymer-based microgels/nanogels for drug delivery applications. In , *1. Stimuli responsive polymeric nanocarriers for drug delivery applications* (pp. 453–500). Elsevier. https://doi.org/10.1016/B978-0-08-101997-9.00021-7.
Viel, S., Capitani, D., Mannina, L., & Segre, A. (2003). Diffusion-ordered NMR spectroscopy: A versatile tool for the molecular weight determination of uncharged polysaccharides. *Biomacromolecules, 4*, 1843–1847. https://doi.org/10.1021/bm0342638
Wang, B., Song, Q., Zhao, F., Zhang, L., Han, Y., & Zhou, Z. (2019). Isolation and characterization of dextran produced by *Lactobacillus sakei* L3 from Hubei sausage. *Carbohydrate Polymers, 223*, Article 115111. https://doi.org/10.1016/j.carbpol.2019.115111
Wang, J. C., & Kinsella, J. E. (1976). Functional properties of novel proteins: Alfalfa leaf *protein. Journal of Food Science, 41*, 286–292. https://doi.org/10.1111/j.1365-2621.1976.tb00602.x
Wang, Y., Sorvali, P., Laitila, A., Maina, N. H., Coda, R., & Katina, K. (2018). Dextran produced *in situ* as a tool to improve the quality of wheat-faba bean composite bread. *Food Hydrocolloids, 84*, 396–405. https://doi.org/10.1016/j.foodhyd.2018.05.042
Wang, Z.-M., Cheung, Y.-C., Leung, P.-H., & Wu, J.-Y. (2010). Ultrasonic treatment for improved solution properties of a high-molecular weight exopolysaccharide produced by a medicinal fungus. *Bioresource Technology, 101*, 5517–5522. https://doi.org/10.1016/j.biortech.2010.01.134
Xing, H., Du, R., Zhao, F., Han, Y., Xiao, H., & Zhou, Z. (2018). Optimization, chain conformation and characterization of exopolysaccharide isolated from *Leuconostoc mesenteroides* DRP105. *International Journal of Biological Macromolecules, 112*, 1208–1216. https://doi.org/10.1016/j.ijbiomac.2018.02.068
Yang, Y., Feng, F., Zhou, Q., Zhao, F., Du, R., Zhou, Z., & Han, Y. (2018). Isolation, purification and characterization of exopolysaccharide produced by *Leuconostoc pseudomesenteroides* YF32 from soybean paste. *International Journal of Biological Macromolecules, 114*, 529–535. https://doi.org/10.1016/j.ijbiomac.2018.03.162
Yang, Y., Peng, Q., Guo, Y., Han, Y., Xiao, H., & Zhou, Z. (2015). Isolation and characterization of dextran produced by *Leuconostoc citreum* NM105 from manchurian sauerkraut. *Carbohydrate Polymers, 133*, 365–372. https://doi.org/10.1016/j.carbpol.2015.07.061
Yilmaz, M. T., İspirli, H., Taylan, O., Taşdemir, V., Sagdic, O., & Dertli, E. (2022). Characterisation and functional roles of a highly branched dextran produced by a bee pollen isolate *Leuconostoc mesenteroides* BI-20. *Food Bioscience, 45*, 2212–4292. https://doi.org/10.1016/j.fbio.2021.101330
Zhou, Q., Feng, F., Yang, Y., Zhao, F., Du, R., Zhou, Z., & Han, Y. (2018). Characterization of a dextran produced by *Leuconostoc pseudomesenteroides* XG5 from homemade wine. *International Journal of Biological Macromolecules, 107*, 2234–2241. https://doi.org/10.1016/j.ijbiomac.2017.10.098